Electrical Power and Energy Systems 155 (2024) 109550

Contents lists available at ScienceDirect

International Journal of Electrical Power and Energy Systems

journal homepage: www.elsevier.com/locate/ijepes

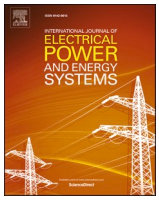

Robust post-disaster repair crew dispatch for distribution systems considering the uncertainty of switches

Hao Zhu, Haipeng Xie *, Lingfeng Tang, Wei Fu, Jianlong Gao

State Key Laboratory of Electrical Insulation and Power Equipment, Department of Electrical Engineering, Xi'an Jiaotong University, Xi'an, Shaanxi 710049, China

ARTICLE INFO

Keywords:
Resilience
Distribution system
Repair crew dispatch
Uncertainty of remote-controlled switches
Tri-level robust model

ABSTRACT

After natural disasters' strike, the remote-controlled switch plays a key role in network reconfiguration to restore the critical load. However, the status of these switches is hardly acquired in case of cyber malfunctions. This paper proposes a robust repair crew dispatch approach for distribution systems considering the uncertainty of remote-controlled switches. The proposed approach is formulated as a tri-level robust optimization model to obtain the repair crew dispatch strategy applicable to possible fault scenarios. The system operator determines the repair crew dispatch scheme at the first level. At the second level, the real-time status of switches under different combinations of faults and repair processes is modeled and the worst fault scenario is calculated. Based on the real-time status of switches, the operator utilizes distributed generators and network reconfiguration to restore loads. A nested column-and–constraint generation (NC&CG) algorithm is customized for the proposed robust model to achieve the optimal solution. Simulation results on the IEEE-33 node distribution test system and the IEEE 123-node system show the proposed approach can effectively reduce the maximum system loss and the NC&CG algorithm can significantly reduce the computing time.

1. Introduction

With global climate change, the frequency of natural disasters has increased significantly, resulting in more power outages and huge economic losses [1–2]. In September 2022, Super Typhoon Nanmadol hit Japan's Kyushu region and caused a power outage for 290 thousand households. In the U.S., more than 80 % of power outages were caused by severe weather events [3], and the failure of distribution systems is the main cause of these power outages [4]. Due to the low strength of the distribution network, it is more vulnerable than the transmission network. Furthermore, most of the distribution networks are radial, which makes them more prone to a power outage after the component failure. Therefore, it is crucial for power supply reliability to improve the resilience of the distribution system against natural disasters.

The post-disaster restoration process directly affects the outage time and load loss of the distribution network. Thereby, fast restoration is important for the distribution system resilience enhancement. Network reconfiguration plays a prominent role in the restoration process. Plenty of research work has been conducted on network reconfiguration in the distribution system restoration. In order to minimize total cost of the system during the storm, a bi-level network reconfiguration model based on pre-storm operational constraints and post-storm operational constraints was proposed in [5]. In [6], Liu et.al proposed a multi-stage restoration method which utilized proactive islanding and fast fault isolation to resist extreme events. Considering the difference of manual switches and remote-controlled switches, Liu et.al proposed a unified two-stage reconfiguration method in [7] to determine the placement of remote-controlled switches and perform network reconfiguration for fast load restoration. To reduce the costs of switching operations, Sabouhi et.al proposed a bi-level optimization with two conflicting objectives in [8] to maximize the resilience of the distribution network and minimize the number of switching operations. In addition to fault isolation, distribution system operators can use network reconfiguration to divide the distribution network into multiple microgrids supported by distributed power sources. The role of microgrids in improving the resilience of power systems was studied in [9–11]. Furthermore, combining network reconfiguration with flexible resources such as distributed power sources(DERs) can significantly improve the recovery effect. In [12], network reconfiguration and DERs scheduling were utilized to respond to the power outage. Based on the work in [12], Shi et.al collaboratively optimized the repair crew dispatch and network reconfiguration to reduce the operating cost in [13]. Furthermore, the increase of mobile power sources in distribution networks provides more

* Corresponding author.
E-mail address: haipengxie@xjtu.edu.cn (H. Xie).

https://doi.org/10.1016/j.ijepes.2023.109550
Received 25 May 2023; Received in revised form 9 August 2023; Accepted 27 September 2023
Available online 8 October 2023

Nomenclature

T	set of time period
N_B	set of nodes
N_F	set of components faults and repair depots
N_{FS}	set of switch faults and repair depots
N_L	set of lines
N_S	set of switches
N_G	set of generators
N_C	set of component repair crews
N_{CS}	set of switch repair crews
$\sigma(j)$	set of lines starting from node j
$\delta(j)$	set of lines ending at node j
R	set of potential root nodes

Parameters

w_j	priority weight of the load at node j
P_j^L	active load demand at node j
Q_j^L	reactive load demand at node j
pf_j	power factor at node j
r_l/X_l	resistance/reactance of line l
S_l^{max}	the capacity of line l
$V_{min,j}/V_{max,j}$	minimum/maximum voltage at node j
$P_{max,g}^G$	maximum active power output of generator g
$Q_{max,g}^G$	maximum reactive power output of generator g
n_b	the number of nodes in the distribution system
$t_{m,c}^{re}$	repair time for crew c to fix component m
t_I^{re}/t_{II}^{re}	repair time of fault I/ fault II
$t_{m,n,c}^{tr}$	travel time for crew c to move from component m to component n
M	a large constant
ε	a small constant

Variables

$P_{l,t}/Q_{l,t}$	active/reactive power flow on line l at time step t
$P_{j,t}^G/Q_{j,t}^G$	active /reactive power output of generator at node j at time step t
$P_{j,t}^{shed}/Q_{j,t}^{shed}$	active/reactive load shedding at node j at time step t
$V_{j,t}$	voltage at node j at time step t
$q_{l,t}$	binary variable equals 1 if line l is closed
$q_{l,t}^{ch}$	binary variable equals 1 if the line status changes
$f_{l,t}$	fictitious power flow on line l at time step t
$\xi_{j,t}$	binary variable equals 1 if node j is a root node
$x_{m,n,c}$	binary variable equals 1 if crew c moves from component m to component n
$y_{m,c}$	binary variable equals 1 if component m is repaired by crew c
$t_{m,c}^{ar}$	arrival time of crew c at component m
$\varphi_{m,t}$	binary variable equals 1 if repair crew c arrive at component m
$z_{m,t}$	binary variable equals 1 if repair crew c has arrived at component m
$\tau_{m,t}$	binary variable equals 1 if component m is repaired at time step t
$\mu_{m,t}$	binary variable equals 1 if component m is available at time step t
$\lambda_{I,m,c}/\lambda_{II,m,c}$	Binary variable equals 1 if repair crew c performs repair process I/II at fault m

flexibility for the post-disaster restoration. In [14], Wang et.al proposed an interesting idea of a separate mobile energy storage system and modeled the fuel delivery issue. Then, the mobile energy resource and the dynamic network reconfiguration cooperated with each other to restore loads. In addition to the grid side, measures taken by the user side also have a significant impact on the restoration process. In [15–16], demand response programs were employed to cooperate with microgrid formation and increase the flexibility of the restoration process. In these studies, the distribution system operator changed the system topology through remote-controlled switches. However, the above methods were proposed on the basis that the distribution system can perform network reconfiguration normally, and the damage to remote-controlled switches was ignored.

Components and switches may be destroyed within a short period of time in case of extreme weather events, such as the typhoon. The damage caused by extreme events to the distribution network is shown in Fig. 1. Notably, extreme events will affect the communication devices and action mechanism of switches. The failure of action mechanism can be regarded as a conventional component failure, such as the line damage. However, the communication fault, such as communication

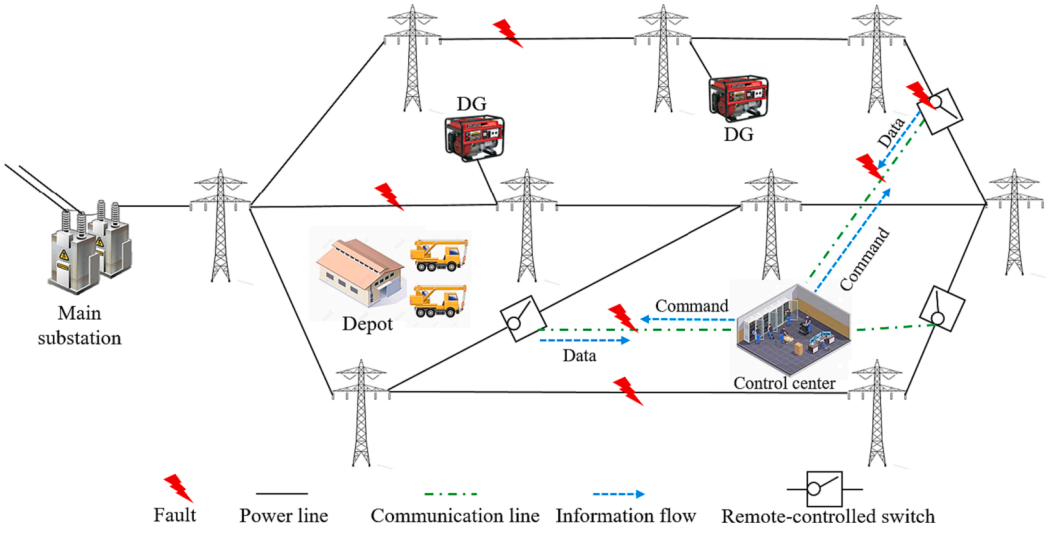

Fig. 1. Impact of extreme events on the distribution network.

link failure [17], will cause the uncontrollable action and the unobservable status. In terms of the uncontrollable action, part of switches cannot receive the command from the control center under communication interruption. The system operator cannot remotely control these switches until they are repaired. The unavailability of switches will restrict the network reconfiguration and affect the efficiency of restoration. In terms of the unobservable status, since the monitoring data of remote-controlled switches cannot be uploaded to the control center, the fault information of switches is unknown to the distribution system operator. Although the system operator can obtain the position of faults through fault indicators and the fault location system [18–20], the unknown fault type will greatly increase the uncertainty and complexity of repair crew dispatch.

Facing the uncertainty in the restoration, stochastic programming is widely used in decision making. However, there are a few practical limitations in stochastic programming: 1) it is difficult for power systems to obtain the accurate probability distribution for all random variables; 2) the large number of scenarios results in difficult calculations [21–23]. In addition, natural disasters have high randomness. Even if the probability of some fault scenarios is very small, they may still occur in disasters. When the actual disaster differs from the predicted disaster, the decision may become invalid. To overcome these limitations, robust optimization has become another option to deal with the uncertainty in the power system resilience enhancement [24]. Generally, the robust approach optimizes the restoration process under the worst scenario, which does not require accurate scenario probability and disaster information. In [25], Yan et.al proposed a two-stage robust model to manage the effects of ice storm forecast errors on both power distribution and urban transportation networks. In [26], Lei et.al proposed a two-stage framework and constructed a robust optimization model to schedule mobile power sources. The collaborative restoration of repair crews and multiple distribution system resources is formulated as a robust optimization model in [27–29]. In these studies, the status of components and switches are assumed to be known after extreme events. To address the unknown line status after extreme events, Sedgh et.al managed the uncertainty of branches status in damaged areas by a two-stage robust optimization model in [30]. However, the work in [30] did not consider the fault of remote-controlled switches and paid less attention to the uncertainty of the fault type.

During the restoration process, network reconfiguration is leveraged to cooperate with the repair crew to restore critical loads. The fault of remote-controlled switches will greatly restrict the network reconfiguration and affect the restoration efficiency. Therefore, the fault of remote-controlled switches deserves more attention. Furthermore, the uncertainty of the fault type will result in an unknown recovery time for the switch, which increases the complexity of repair resources scheduling. The improper scheduling may be ineffective or even counterproductive. The repair crew dispatch with incomplete fault information is becoming an operational challenge faced by the system operator. It is necessary to develop a general scheduling method suitable for most fault scenarios.

To overcome the aforementioned challenge, this paper proposes a robust distribution system restoration method considering the fault of components and remote-controlled switches. The main contributions of this paper can be summarized as follows:

(1) A resilience-oriented robust repair crew dispatch approach towards the uncontrollability and unobservability of remote-controlled switches for the distribution system is proposed. The approach considers all possible fault scenarios and develops a universal repair crew scheduling strategy suitable for all scenarios to prevent excessive system losses.
(2) The proposed approach is formulated as a tri-level robust optimization model to address the uncertainty of the switch fault. The real-time status of switches under different combinations of faults and repair processes is modeled. The distributed generator(DG) scheduling and network reconfiguration are involved.
(3) To effectively solve the proposed tri-level robust model, a customized NC&CG algorithm is employed to achieve the global optimal solution and reduce the computing time.

The rest of this paper is organized as follows. Section 2 presents the robust repair crew dispatch approach. Section 3 formulates the tri-level robust optimization model for the restoration. The customized NC&CG algorithm is presented in Section 4. Section 5 presents the case results, and conclusions are drawn in Section 6.

2. Robust repair crew dispatch approach

Due to the relatively lower design strength, the distribution system is vulnerable to extreme events. The component failure caused by extreme events will result in power supply outages to the load. After the power supply is interrupted, the system operator will restore the critical load through repair crew dispatch, DG scheduling and network reconfiguration. The fault of remote-controlled switches will restrict network reconfiguration. Due to the high coupling between component repair and network reconfiguration, repair crews may need to change the sequence of component maintenance.

To find a scheduling plan which can deal with all possible fault scenarios, this paper proposes a robust repair crew dispatch approach. Since different repair skills are required for the component maintenance and the switch maintenance, repair crews are divided into the component repair crew (CRC) and the switch repair crew (SRC). With the development of fault location techniques, the distribution system can quickly obtain the fault location after extreme events. The action mechanism failure of switches can be regarded as a conventional component failure. Therefore, this paper only considers two types of switch fault: (I) the communication device is damaged and the action mechanism is intact; (II) both the communication device and the action mechanism are damaged. The detailed fault location of communication devices is often more difficult to find, so the switch maintenance requires more time. The repair processes corresponding to the above faults are Repair I and Repair II, respectively. Different switch fault combinations result in different repair crew dispatch plans. Facing the unknown fault combinations, the operator needs to make the most robust decision. The proposed robust repair crew dispatch approach is presented by Fig. 2. Although the distribution system lacks sufficient historical data to obtain the probability of each combinations, it is possible to predict the maximum number of fault I and fault II. In the decision stage, considering all possible fault combinations, the operator arranges the maintenance sequence and the repair process at each fault switch to reduce the maximum load loss. During the implementation stage, CRCs and SRCs repair faults according to the sequence in the restoration plan. Since the robust scheduling is mainly for the worst scenario, the planned repair process at each fault switch may not match the actual fault type. When SRCs reach the fault switch, the fault type will become known and the repair process will be corrected to the corresponding process.

Explanation: *After the repair sequence is determined, the distribution system operator just needs to adjust the output of DGs and perform network reconfiguration according to the real-time status of components and switches. The implementation stage is essentially a distributed power resource scheduling problem, which has been studied in* [5–15]. *Therefore, this paper only focuses on the decision stage and the repair sequence of components and switches.*

3. Tri-level robust optimization model

In this section, the proposed robust repair crew dispatch approach is formulated as a tri-level MILP model to optimize the repair crew dispatch, DG scheduling and network reconfiguration.

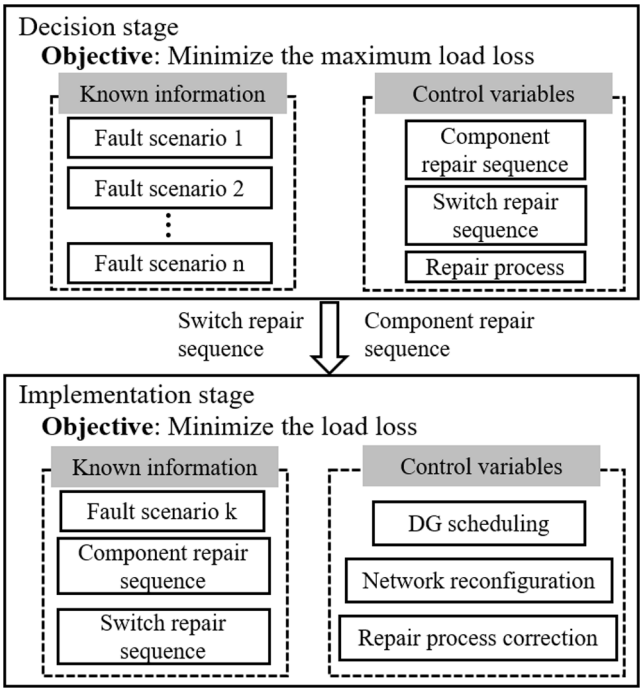

Fig. 2. The proposed robust repair crew dispatch approach.

3.1. Objective function

$$\min_{x_{\mathrm{CRC}}\in\chi_{\mathrm{CRC}},x_{\mathrm{SRC}}\in\chi_{\mathrm{SRC}}}\max_{a\in A}\min_{q\in\varsigma}\sum_{t\in T}\sum_{j\in N_{\mathrm{B}}}w_j P_{j,t}^{\mathrm{shed}} \tag{1}$$

where χ_{CRC} represents the set of all CRC scheduling strategies. χ_{SRC} is the set of all SRC scheduling strategies.A represents all combinations of switch faults. ς is the set of all network reconfiguration schemes. The objective function is to minimize the loss of weighted loads under the worst combination of switch faults.

3.2. Distribution system operational constraints

The power flow model can be represented by the linearized DistFlow model[31], which is as follows:

$$\sum_{l\in\sigma(j)}P_{l,t}-\sum_{l\in\delta(j)}P_{l,t}=P_{j,t}^{G}-\left(P_{j}^{L}-P_{j,t}^{\mathrm{shed}}\right),\forall t\in T,\forall j\in N_{\mathrm{B}} \tag{2}$$

$$\sum_{l\in\sigma(j)}Q_{l,t}-\sum_{l\in\delta(j)}Q_{l,t}=Q_{j,t}^{G}-\left(Q_{j}^{L}-Q_{j,t}^{\mathrm{shed}}\right),\forall t\in T,\forall j\in N_{\mathrm{B}} \tag{3}$$

$$V_{i,t}-V_{j,t}-\left(r_l P_{l,t}+X_l Q_{l,t}\right)/V_0\leqslant M\left(1-q_{l,t}\right),\forall t\in T,\forall l\in N_{\mathrm{L}} \tag{4}$$

$$V_{i,t}-V_{j,t}-\left(r_l P_{l,t}+X_l Q_{l,t}\right)/V_0\geqslant -M\left(1-q_{l,t}\right),\forall t\in T,\forall l\in N_{\mathrm{L}} \tag{5}$$

$$V_{\min,j}^{2}\leqslant V_{j,t}\leqslant V_{\max,j}^{2},\forall t\in T,\forall j\in N_{\mathrm{B}} \tag{6}$$

$$0\leqslant P_{j,t}^{G}\leqslant P_{\max,j}^{G},\forall t\in T,\forall j\in N_{\mathrm{B}} \tag{7}$$

$$0\leqslant Q_{j,t}^{G}\leqslant Q_{\max,j}^{G},\forall t\in T,\forall j\in N_{\mathrm{B}} \tag{8}$$

$$-q_{l,t}S_{l}^{\max}\leqslant P_{l,t}\leqslant q_{l,t}S_{l}^{\max},\forall t\in T,\forall l\in N_{\mathrm{L}} \tag{9}$$

$$-q_{l,t}S_{l}^{\max}\leqslant Q_{l,t}\leqslant q_{l,t}S_{l}^{\max},\forall t\in T,\forall l\in N_{\mathrm{L}} \tag{10}$$

$$0\leqslant P_{j,t}^{\mathrm{shed}}\leqslant P_{j}^{L},\forall t\in T,\forall j\in N_{\mathrm{B}} \tag{11}$$

$$Q_{j,t}^{\mathrm{shed}}=P_{j,t}^{\mathrm{shed}}\Big/pf_j,\forall t\in T,\forall j\in N_{\mathrm{B}} \tag{12}$$

Constraints (2) and (3) represent the active and reactive power flow balance constraints respectively. The voltage at each node can be described by constraints (4) and (5), where V_0 is the reference voltage. Constraint (6) restricts the voltage amplitude at each node. The active and reactive output of each generator are limited by constraints (7) and (8), respectively. Constraints (9) and (10) define the active and reactive power flow limits. When the line is damaged or manually disconnected, the power flowing through the line should be zero. Constraint (11) indicates that the load shedding cannot exceed the original load at each node. Constraint (12) ensures that the power factor of each node remains constant during the restoration process.

3.3. CRC dispatch constraints

The CRC dispatch is essentially a vehicle-routing problem (VRP) [32]. Binary variables x and y are used for the repair crew dispatch:

$$x_{m,n,c}=\begin{cases}1, & \text{crew } c \text{ travels from node } m \text{ to node } n\\ 0, & \text{otherwise}\end{cases}$$

$$y_{m,c}=\begin{cases}1, & \text{crew } c \text{ has arrived at node } m\\ 0, & \text{otherwise}\end{cases}$$

The CRC dispatch constraints are expressed as follows:

$$\sum_{n\in N_{\mathrm{F}}\backslash\{dp\}}x_{dp,n,c}-\sum_{n\in N_{\mathrm{F}}\backslash\{dp\}}x_{n,dp,c}=1,\forall c\in N_{\mathrm{C}} \tag{13}$$

$$\sum_{n\in N_{\mathrm{F}}\backslash\{m\}}x_{m,n,c}-\sum_{n\in N_{\mathrm{F}}\backslash\{m\}}x_{n,m,c}=0,\forall c\in N_{\mathrm{C}},\forall m\in N_{\mathrm{F}}\backslash\{dp,ds\} \tag{14}$$

$$\sum_{n\in N_{\mathrm{F}}\backslash\{dp,ds\}}x_{ds,n,c}-\sum_{n\in N_{\mathrm{F}}\backslash\{dp,ds\}}x_{n,ds,c}=-1,\forall c\in N_{\mathrm{C}} \tag{15}$$

$$\sum_{c\in N_{\mathrm{C}}}y_{m,c}=1,\forall m\in N_{\mathrm{F}}\backslash\{dp\} \tag{16}$$

$$y_{m,c}=\sum_{\forall n\in N_{\mathrm{F}}\backslash\{m\}}x_{n,m,c},\forall m\in N_{\mathrm{F}}\backslash\{dp\} \tag{17}$$

$$-M\left(1-x_{m,n,c}\right)\leqslant t_{m,c}^{ar}+t_{m}^{re}+t_{m,n,c}^{tr}-t_{n,c}^{ar}\leqslant M\left(1-x_{m,n,c}\right),\forall m,n\in N_F,\forall c\in N_C \tag{18}$$

$$0\leqslant t_{m,c}^{\mathrm{ar}}\leqslant My_{m,c},\forall c\in N_{\mathrm{C}},\forall m\in N_{\mathrm{F}} \tag{19}$$

where dp and ds represent repair depots. Constraint (13) ensures that repair crews start from the repair depot. Constraint (14) enforces repair crews leave damaged components after they have been repaired. Constraint (15) means that all repair crews must return to the repair depot. Constraints (16) and (17) ensure that each damaged component is repaired by a repair crew. Constraints (18) and (19) can obtain the time for repair crews to arrive at each damaged component.

Furthermore, it is critical to obtain the status of the damaged components during the restoration. Binary variables φ and z are introduced to represent the arrival of the repair crew. Binary variables τ and μ are used to obtain the component status, as shown in Fig. 3.τ is equal to 1 at the moment after the component is repaired, and 0 at other time. μ is equal to 1 when the component is in normal status, and 0 when it is in any other status.

The abovementioned binary variables are expressed by the following constraints:

$$\sum_{\forall t\in T}t\varphi_{m,t}\geqslant\sum_{\forall c\in N_{\mathrm{C}}}t_{m,c}^{\mathrm{ar}},\forall m\in N_{\mathrm{F}} \tag{20}$$

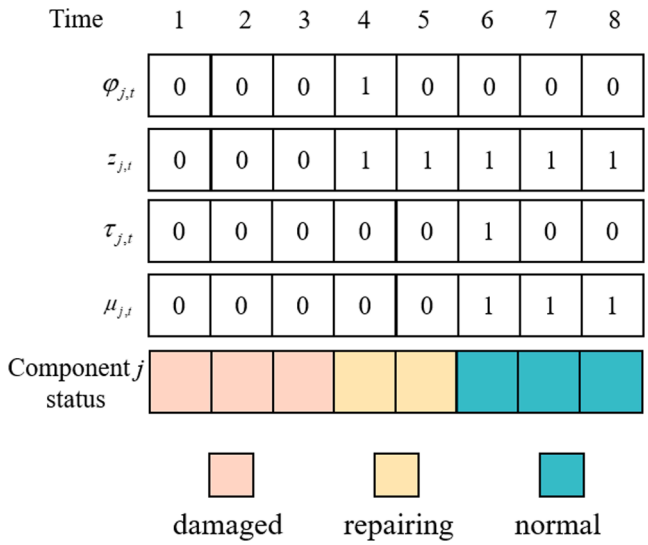

Fig. 3. Example for binary variables φ, Z, τ, z and μ.

$$\sum_{\forall t\in T} t\varphi_{m,t} \leqslant 1-\varepsilon+\sum_{\forall c\in N_C} t^{\mathrm{ar}}_{m,c}, \forall m\in N_F \tag{21}$$

$$z_{m,t} \leqslant \sum_{o=1}^{t} \varphi_{m,o}, \forall m\in N_F, \forall t\in T \tag{22}$$

$$\sum_{\forall t\in T} t\tau_{m,t} \geqslant \sum_{\forall c\in N_C} \left(t^{\mathrm{ar}}_{m,c}+t^{\mathrm{re}}_{m,c}y_{m,c}\right), \forall m\in N_F \tag{23}$$

$$\sum_{\forall t\in T} t\tau_{m,t} \leqslant 1-\varepsilon+\sum_{\forall c\in N_C} \left(t^{\mathrm{ar}}_{m,c}+t^{\mathrm{re}}_{m,c}y_{m,c}\right), \forall m\in N_F \tag{24}$$

$$\mu_{m,t} \leqslant \sum_{o=1}^{t} \tau_{m,o}, \forall m\in N_F, \forall t\in T \tag{25}$$

The status of components can be expressed as follows:

$$q_{m,t}=\mu_{m,t}, \forall m\in N_F\backslash\{dp,ds\} \tag{26}$$

$$q_{l,t}=1, \forall l\in N_L\backslash\{N_F\cup N_S\}, \forall t\in T \tag{27}$$

3.4. SRC dispatch constraints

Likewise, the SRC dispatch is also expressed in the form of (13) - (25). However, the repair time of switches is uncertainty. Therefore, the constraints (18), (23) and (24) are rewritten as follows:

$$-M\left(1-x_{m,n,c}\right) \leqslant t^{\mathrm{ar}}_{m,c}+t^{\mathrm{re}}_{\mathrm{I}}\lambda_{\mathrm{I},m,c}+t^{\mathrm{re}}_{\mathrm{II}}\lambda_{\mathrm{II},m,c}+t^{\mathrm{tr}}_{m,n,c}-t^{\mathrm{ar}}_{n,c} \leqslant M\left(1-x_{m,n,c}\right), \forall m,n\in N_{\mathrm{FS}}, \forall c\in N_{\mathrm{CS}} \tag{28}$$

$$\sum_{\forall t\in T} t\tau_{m,t} \geqslant \sum_{\forall c\in N_{\mathrm{CS}}} \left(t^{\mathrm{ar}}_{m,c}+t^{\mathrm{re}}_{\mathrm{I}}\lambda_{\mathrm{I},m,c}+t^{\mathrm{re}}_{\mathrm{II}}\lambda_{\mathrm{II},m,c}\right), \forall m\in N_{\mathrm{FS}} \tag{29}$$

$$\sum_{\forall t\in T} t\tau_{m,t} \leqslant 1-\varepsilon+\sum_{\forall c\in N_{\mathrm{CS}}} \left(t^{\mathrm{ar}}_{m,c}+t^{\mathrm{re}}_{\mathrm{I}}\lambda_{\mathrm{I},m,c}+t^{\mathrm{re}}_{\mathrm{II}}\lambda_{\mathrm{II},m,c}\right), \forall m\in N_{\mathrm{FS}} \tag{30}$$

$$\lambda_{\mathrm{I},m,c}+\lambda_{\mathrm{II},m,c}=1, \forall m\in N_{\mathrm{FS}}, \forall c\in N_{\mathrm{CS}} \tag{31}$$

where binary variables $\lambda_{\mathrm{I},m,c}$ and $\lambda_{\mathrm{II},m,c}$ represent the Repair I and Repair II, respectively. If fault I occurs at switch m, $a_{\mathrm{I},m}$ is equal to 0, otherwise 1. Likewise, $a_{\mathrm{II},m}$ is equal to 0 when fault II occurs at switch m.

The status under different combinations of the fault type and the repair process are shown in Fig. 4. For fault I, although the switch cannot be controlled remotely by the distribution system operator, it can be operated manually by the SRC. Therefore, the switch with fault I is available after the SRC arrives. The switch with fault II cannot be operated until it is repaired. To obtain the worst scenario, the fault

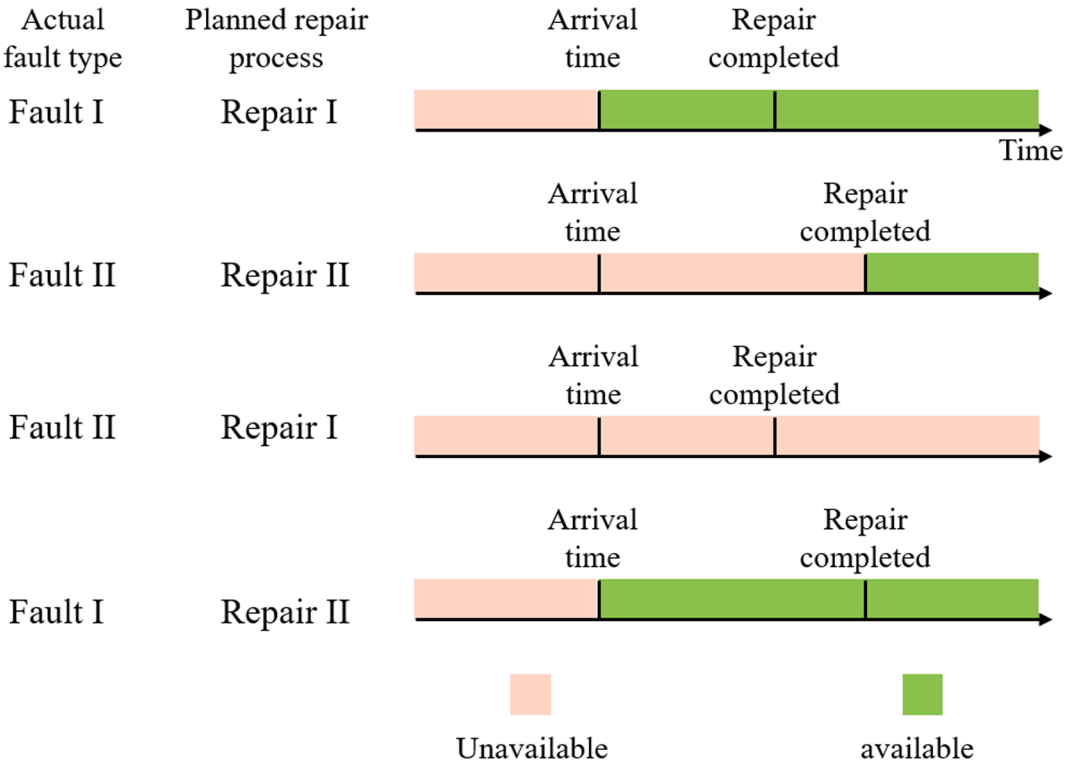

Fig. 4. Switch status under different combinations of the fault type and the repair process.

switch is unavailable during the whole restoration process if fault II occurs and the planned repair process is Repair I.

The status of fault switches can be represented by:

$$q_{m,t}^{\mathrm{ch}} \leqslant (1-a_{\mathrm{I},m}) z_{m,t} \sum_{c\in N_{\mathrm{CS}}} \lambda_{\mathrm{I},m,c} + (1-a_{\mathrm{II},m}) \mu_{m,t} \sum_{c\in N_{\mathrm{CS}}} \lambda_{\mathrm{II},m,c} + (1 - a_{\mathrm{II},m}) z_{m,t} \sum_{c\in N_{\mathrm{CS}}} \lambda_{1,m,c}, \forall m \in N_{\mathrm{FS}} \backslash \{dp, ds\}, \forall t \in T \backslash \{1\} \tag{32}$$

$$q_{l,t}^{\mathrm{ch}} = |q_{l,t} - q_{l,t-1}|, \forall t \in T \backslash \{1\}, \forall l \in N_{\mathrm{S}} \tag{33}$$

Constraints (32) and (33) can be linearized by:

$$q_{m,t}^{\mathrm{ch}} \leqslant e_{m,t}^{1} + e_{m,t}^{2} + e_{m,t}^{3}, \forall m \in N_{FS}, \forall t \in T \backslash \{1\} \tag{34}$$

$$\begin{cases} e_{m,t}^{1} \leqslant e_{m,t}^{4}, e_{m,t}^{1} \leqslant \sum_{c\in N_{\mathrm{CS}}} \lambda_{1,m,c}, e_{m,t}^{1} \geqslant e_{m,t}^{4} + \sum_{c\in N_{\mathrm{CS}}} \lambda_{1,m,c} - 1 \\ e_{m,t}^{2} \leqslant e_{m,t}^{5}, e_{m,t}^{2} \leqslant \sum_{c\in N_{\mathrm{CS}}} \lambda_{\mathrm{II},m,c}, e_{m,t}^{2} \geqslant e_{m,t}^{5} + \sum_{c\in N_{\mathrm{CS}}} \lambda_{\mathrm{II},m,c} - 1 \\ e_{m,t}^{3} \leqslant e_{m,t}^{6}, e_{m,t}^{3} \leqslant \sum_{c\in N_{\mathrm{CS}}} \lambda_{1,m,c}, e_{m,t}^{3} \geqslant e_{m,t}^{6} + \sum_{c\in N_{\mathrm{CS}}} \lambda_{1,m,c} - 1 \end{cases} \tag{35}$$

$$\begin{cases} e_{m,t}^{4} \leqslant 1 - a_{\mathrm{I},m}, e_{m,t}^{4} \leqslant z_{m,t}, e_{m,t}^{4} \geqslant z_{m,t} - a_{\mathrm{I},m} \\ e_{m,t}^{5} \leqslant 1 - a_{\mathrm{II},m}, e_{m,t}^{5} \leqslant \mu_{m,t}, e_{m,t}^{5} \geqslant \mu_{m,t} - a_{\mathrm{II},m} \\ e_{m,t}^{6} \leqslant 1 - a_{\mathrm{II},m}, e_{m,t}^{6} \leqslant z_{m,t}, e_{m,t}^{6} \geqslant z_{m,t} - a_{\mathrm{II},m} \end{cases} \tag{36}$$

$$q_{l,t}^{\mathrm{ch}} \geqslant q_{l,t} - q_{l,t-1}, q_{l,t}^{\mathrm{ch}} \geqslant q_{l,t-1} - q_{l,t}, q_{l,t}^{\mathrm{ch}} \leqslant q_{l,t-1} + q_{l,t}, q_{l,t}^{\mathrm{ch}} \leqslant 2 - q_{l,t-1} - q_{l,t} \forall t \in T \backslash \{1\}, \forall l \in N_{\mathrm{S}} \tag{37}$$

3.5. Topology reconfiguration constraints

The distribution network must be operated radially. According to the graph theory, a radiant graph must satisfy two conditions: (i) the number of edges is equal to the number of nodes minus the number of subgraphs; (ii) each subgraph must guarantee the connectivity. The condition (i) is given by constraint (38). Constraints (39)-(41) can guarantee the connectivity of subgraphs. These two conditions are formulated as the following constraints[33]:

$$\sum_{l\in N_{\mathrm{L}}} q_{l,t} = n_b - \sum_{j\in R} \xi_{j,t}, \forall t \in T \tag{38}$$

$$\sum_{l\in\delta(j)} f_{l,t} - \sum_{l\in\sigma(j)} f_{l,t} = 1, \forall t \in T, \forall j \in N_{\mathrm{B}} \backslash R \tag{39}$$

$$1 - M\xi_{j,t} \leqslant \sum_{l\in\delta(j)} f_{l,t} - \sum_{l\in\sigma(j)} f_{l,t} \leqslant 1 + M\xi_{j,t}, \forall t \in T, \forall j \in R \tag{40}$$

$$-Mq_{l,t} \leqslant f_{l,t} \leqslant Mq_{l,t}, \forall t \in T, \forall l \in N_{\mathrm{L}} \tag{41}$$

3.6. The final tri-level restoration model

Based on the above models, the final tri-level robust restoration model is formed as:

Obj: (1)

$$\text{s.t. } a_{\mathrm{I},m} + a_{\mathrm{II},m} = 1, \forall m \in N_{\mathrm{FS}} \backslash \{dp, ds\} \tag{42}$$

$$\sum_{m\in N_{\mathrm{FS}}\backslash\{dp,ds\}} (1 - a_{\mathrm{II},m}) \leqslant a_{\mathrm{II}}^{\max} \tag{43}$$

Operational constraints: (2)-(12)
CRC dispatch constraints: (13) - (25)
SRC dispatch constraints: (13)-(17), (19)-(22), (25), (28)-(31), replace sets N_{F} and N_{C} with N_{FS} and N_{CS}.
Topology constraints: (26)-(27), (34)-(41)

The maximum number of fault II is similar to the maximum number of damaged lines in 'N-k' problem. Before the disaster, the distribution system can receive forewarning from the emergency management department. The distribution system can predict the maximum number of faults based on the disaster intensity and historical data[34–35]. To simplify the following expression, the above constraints are rewritten in the matrix form:

Operational constraints: $\boldsymbol{D\zeta \leqslant b}$
CRC dispatch constraints: $\boldsymbol{Ex}_{\mathrm{CRC}} \boldsymbol{\leqslant g}$
SRC dispatch constraints: $\boldsymbol{F x}_{\mathrm{SRC}} \boldsymbol{\leqslant h}$
Topology constraints: $\boldsymbol{Hv} + \boldsymbol{J}\begin{bmatrix} \boldsymbol{x}_{\mathrm{CRC}} \\ \boldsymbol{x}_{\mathrm{SRC}} \end{bmatrix} + \boldsymbol{K}\begin{bmatrix} \boldsymbol{a}_{\mathrm{I}} \\ \boldsymbol{a}_{\mathrm{II}} \end{bmatrix} \boldsymbol{\leqslant u}$

4. Customized NC&CG algorithm

Since the restoration process involves repair crew dispatch and network reconfiguration, a large number of 0/1 variables are introduced into the model. The proposed tri-level robust optimization model is essentially a large-scale MILP model. The non-convexity of the model makes it difficult to be directly solved by traditional optimization methods, such as Karush- Kuhn-Tucker (KKT) condition. To address the computational challenge, this paper customizes and employs the nested column-and-constraint generation(NC&CG) method[36–37]. The proposed model is decoupled into the upper level problem (UP), the lower level master problem (LMP) and the lower level sub-problem (LSP), as shown in Fig. 5:

(1) UP: Based on the set of switch faults, the distribution system operator dispatches CRCs and SRCs to minimize the loss of load. The optimal CRC and SRC scheduling is transferred to the lower level problem.
(2) LMP: Under the premise that CRC and SRC scheduling is known, LMP calculates the worst switch fault combination considering

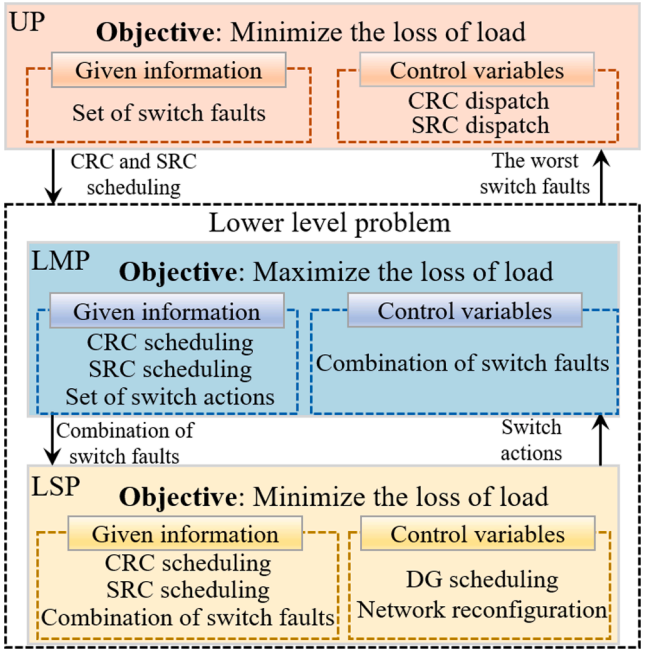

Fig. 5. The upper level problem and lower level problems.

DG scheduling and network reconfiguration to maximize the loss of load. The switch fault combination is transferred to LSP.

(3) LSP: According to the fixed repair crew scheduling and switch faults, LSP minimizes the loss of load by DG scheduling and network reconfiguration.

$$\begin{aligned}\beta_2 \leqslant & -\sum_{t\in T}\sum_{j\in N_B} P_j^L\cdot\eta_{1,j,t}^m - \sum_{t\in T}\sum_{j\in N_B} Q_j^L\cdot\eta_{2,j,t}^m + \sum_{t\in T}\sum_{l\in N_L} M\left(1-q_{l,t}^m\right)\cdot\eta_{3,l,t}^m - \sum_{t\in T}\sum_{l\in N_L} M\left(1-q_{l,t}^m\right)\cdot\eta_{4,l,t}^m \\ & -\sum_{t\in T}\sum_{l\in N_L} S_l^{\max}\cdot q_{l,t}^m\cdot\eta_{5,l,t}^m + \sum_{t\in T}\sum_{l\in N_L} S_l^{\max}\cdot q_{l,t}^m\cdot\eta_{6,l,t}^m - \sum_{t\in T}\sum_{l\in N_L} S_l^{\max}\cdot q_{l,t}^m\cdot\eta_{7,l,t}^m + \sum_{t\in T}\sum_{l\in N_L} S_l^{\max}\cdot q_{l,t}^m\cdot\eta_{8,l,t}^m \\ & +\sum_{t\in T}\sum_{j\in N_B} P_j^L\cdot\eta_{9,j,t}^m + \sum_{t\in T}\sum_{j\in N_B} P_{\max,j}^G\cdot\eta_{10,j,t}^m + \sum_{t\in T}\sum_{j\in N_B} Q_{\max,j}^G\cdot\eta_{11,j,t}^m + \sum_{t\in T}\sum_{j\in N_B} V_{\min,j}^2\cdot\eta_{12,j,t}^m \\ & +\sum_{t\in T}\sum_{j\in N_B} V_{\max,j}^2\cdot\eta_{13,j,t}^m\end{aligned} \tag{53}$$

Notably, the initial switch fault set and switch action set are arbitrary. New elements will be added to them during the iteration. The outer-loop C&CG algorithm is implemented between the UP and the lower level problem to obtain the most robust repair crew scheduling strategy. The inner-loop C&CG algorithm is employed between the LMP and the LSP to find the worst combination of switch faults.

4.1. Upper level problem

The UP is to generate the most robust repair crew scheduling strategy for the switch faults set $\widehat{\boldsymbol{A}}$. $\widehat{\boldsymbol{A}}$ is a finite set whose elements are known. The UP is written as:

$$\min_{\boldsymbol{x}_{\mathrm{CRC}},\boldsymbol{x}_{\mathrm{SRC}},\boldsymbol{\xi},\boldsymbol{v}} \max_{\boldsymbol{a}\in\widehat{\boldsymbol{A}}} \sum_{t\in T}\sum_{j\in N_{\mathrm{B}}} w_j P_{j,t}^{\mathrm{shed}} \tag{44}$$

The UP is reformulated as:

$$\min\beta_1 \tag{45}$$

$$\beta_1 \geqslant \sum_{t\in T}\sum_{j\in N_{\mathrm{B}}} w_j P_{j,t,k}^{\mathrm{shed}}, k=1,2,\ldots \tag{46}$$

$$\boldsymbol{E}\boldsymbol{x}_{\mathrm{CRC}} \leqslant \boldsymbol{g} \tag{47}$$

$$\boldsymbol{F}\boldsymbol{x}_{\mathrm{SRC}} \leqslant \boldsymbol{h} \tag{48}$$

$$\boldsymbol{D}\boldsymbol{\xi}^k \leqslant \boldsymbol{b}, k=1,2,\ldots \tag{49}$$

$$\boldsymbol{H}\boldsymbol{v}^k + \boldsymbol{J}\begin{bmatrix}\boldsymbol{x}_{\mathrm{CRC}}\\ \boldsymbol{x}_{\mathrm{SRC}}\end{bmatrix} + \boldsymbol{K}\begin{bmatrix}\widehat{\boldsymbol{a}}_{\mathrm{I}}^k\\ \widehat{\boldsymbol{a}}_{\mathrm{II}}^k\end{bmatrix} \leqslant \boldsymbol{u}, k=1,2,\ldots \tag{50}$$

where k is the number of iteration for the outer-loop C&CG algorithm. The fault type $\widehat{\boldsymbol{a}}_{\mathrm{I}}^k$ and $\widehat{\boldsymbol{a}}_{\mathrm{II}}^k$ are fixed. The damaged component status $\mu_{l,t}$ and switch repair plan will be transferred to the lower level problem.

4.2. Lower level master problem

Given the CRC and SRC scheduling strategy, the LMP calculates the worst combination of switch faults. The LMP is written as:

$$\max_{\boldsymbol{a}\in\boldsymbol{A}} \min_{\boldsymbol{x}_{\mathrm{CRC}},\boldsymbol{x}_{\mathrm{SRC}},\boldsymbol{\xi},\boldsymbol{v}} \sum_{t\in T}\sum_{j\in N_{\mathrm{B}}} w_j P_{j,t}^{\mathrm{shed}} \tag{51}$$

The LMP is a min–max problem, which is difficult to be solved directly. Therefore, the strong duality theory is applied to transform the LMP into a single-level "max" problem. The variable "$\boldsymbol{\eta}$" is the dual variable corresponding to operational constraints (2)-(12). The detail of "$\boldsymbol{\eta}$" is presented in [37]. The mathematical form of the LMP is as follows:

$$\max\beta_2 \tag{52}$$

s.t. (42)-(43)

$$-\eta_{1,j,t}^m + \eta_{9,j,t}^m - \eta_{14,j,t}^m \Big/ pf_j \leqslant w_j \tag{54}$$

$$-\eta_{2,j,t}^m + \eta_{14,j,t}^m \leqslant 0 \tag{55}$$

$$-\eta_{1,j,t}^m + \eta_{10,j,t}^m \leqslant 0 \tag{56}$$

$$-\eta_{2,j,t}^m + \eta_{11,j,t}^m \leqslant 0 \tag{57}$$

$$\eta_{1,i,t}^m - \eta_{1,j,t}^m - r_l\eta_{3,l,t}^m \Big/ V_0 - r_l\eta_{4,l,t}^m \Big/ V_0 + \eta_{5,l,t}^m + \eta_{6,l,t}^m = 0 \tag{58}$$

$$\eta_{2,i,t}^m - \eta_{2,j,t}^m - x_l\eta_{3,l}^m \Big/ V_0 - x_l\eta_{4,l,t}^m \Big/ V_0 + \eta_{7,l,t}^m + \eta_{8,l,t}^m = 0 \tag{59}$$

$$\sum_{l\in\sigma(j)}\eta_{3,l,t}^m - \sum_{i\in\delta(j)}\eta_{3,l,t}^m + \sum_{s\in\sigma(j)}\eta_{4,l,t}^m - \sum_{i\in\delta(j)}\eta_{4,l,t}^m + \eta_{12,j,t}^m + \eta_{13,j,t}^m = 0 \tag{60}$$

$$\begin{aligned}&\eta_3^m \leqslant 0, \eta_4^m \geqslant 0, \eta_5^m \geqslant 0, \eta_6^m \leqslant 0, \eta_7^m \geqslant 0, \eta_8^m \leqslant 0, \eta_9^m \leqslant 0, \eta_{10}^m \leqslant 0, \\ &\eta_{10}^m \leqslant 0, \eta_{11}^m \leqslant 0, \eta_{12}^m \geqslant 0, \eta_{13}^m \leqslant 0\end{aligned} \tag{61}$$

$$q_{l,t}^m = \widehat{\mu}_{l,t}, \forall l \in N_{\mathrm{F}}\backslash\{dp, ds\} \tag{62}$$

$$q_{l,t}^m = 1, \forall l \in N_L\backslash\{N_F \cup N_S\} \tag{63}$$

$$\begin{aligned}q_{l,t}^{\mathrm{ch},m} = \widehat{q}_{\mathrm{LSP},l,t}^{\mathrm{ch},m}\Bigg(&\left(1-a_{\mathrm{I},l}\right)\widehat{z}_{l,t}^m\sum_{c\in N_{\mathrm{CS}}}\widehat{\lambda}_{\mathrm{I},l,c}^m + \left(1-a_{\mathrm{II},l}\right)\widehat{\mu}_{l,t}^m\sum_{c\in N_{\mathrm{CS}}}\widehat{\lambda}_{\mathrm{II},l,c}^m + \Big(1 \\ &- a_{\mathrm{I},l}\Big)\widehat{z}_{l,t}^m\sum_{c\in N_{\mathrm{CS}}}\widehat{\lambda}_{\mathrm{II},l,c}^m\Bigg), \forall l \\ &\in N_{\mathrm{FS}}\backslash\{dp, ds\}\end{aligned} \tag{64}$$

$$\begin{aligned}&q_{l,t}^{\mathrm{ch},m} \geqslant q_{l,t}^m - q_{l,t-1}^m, q_{l,t}^{\mathrm{ch},m} \geqslant q_{l,t-1}^m - q_{l,t}^m, q_{l,t}^{\mathrm{ch},m} \leqslant q_{l,t-1}^m + q_{l,t}^m, \\ &q_{l,t}^{\mathrm{ch},m} \leqslant 2 - q_{l,t-1}^m - q_{l,t}^m, \forall t \in T\backslash\{1\}, \forall l \in N_{\mathrm{S}}\end{aligned} \tag{65}$$

where m is the number of iterations for the inner-loop C&CG algorithm. $\widehat{q}_{\mathrm{LSP},l,t}^{\mathrm{ch},m}$ represents the switch action during the restoration, which is given by the LSP. The obtained switch fault combination will be transferred to the LSP.

4.3. Lower level sub-problem

After the repair crew scheduling and switch faults are given, the LSP optimizes DG scheduling and network reconfiguration to minimize the loss of load. The mathematical form of the LSP is an MILP model:

$$\min_{\hat{\boldsymbol{x}}_{\mathrm{CRC}},\hat{\boldsymbol{a}},\hat{\boldsymbol{x}}_{\mathrm{SRC}},\boldsymbol{\xi},\boldsymbol{v}} \sum_{t\in T}\sum_{j\in N_{\mathrm{B}}} w_j P_{j,t}^{\mathrm{shed}} \tag{66}$$

$$\boldsymbol{D\zeta} \leqslant \boldsymbol{b} \tag{67}$$

$$\boldsymbol{Hv} + \boldsymbol{J}\begin{bmatrix}\widehat{\boldsymbol{x}}_{\mathrm{CRC}}\\ \widehat{\boldsymbol{x}}_{\mathrm{SRC}}\end{bmatrix} + \boldsymbol{K}\begin{bmatrix}\widehat{\boldsymbol{a}}_{\mathrm{I}}\\ \widehat{\boldsymbol{a}}_{\mathrm{II}}\end{bmatrix} \leqslant \boldsymbol{u} \tag{68}$$

The optimal solution of LSP will be added to the switch action set in the LMP. When the inner-loop C&CG algorithm is completed, the worst switch fault combination found by the LMP will be added to the fault set in the UP. After the outer-loop C&CG algorithm converges, the most robust scheduling strategy is obtained. The detailed flowchart of the NC&CG algorithm is described in Fig. 6.

5. Case study

In this section, the effectiveness of the proposed tri-level robust restoration model is verified in the modified IEEE 33-node test system and the modified IEEE 123-node system. The solution algorithm is implemented in MATLAB R2021a with Gurobi 10.0 on an i7-10700F core PC with 16 GB RAM.

5.1. IEEE 33-node test system

Fig. 7 shows the modified IEEE 33-node test system, which contains 4 DGs and 37 branches. The system load is 3.715 MW + 2.3Mvar. The system voltage is 12.66 kV. 5 lines are installed with remote-controlled switches. The voltage range is 0.9p.u. ~ 1.1p.u. in this system. The maximum output of each DG is 0.2 MW. The repair depot is located at node 10, and there are three repair crews in this depot. 7 lines were

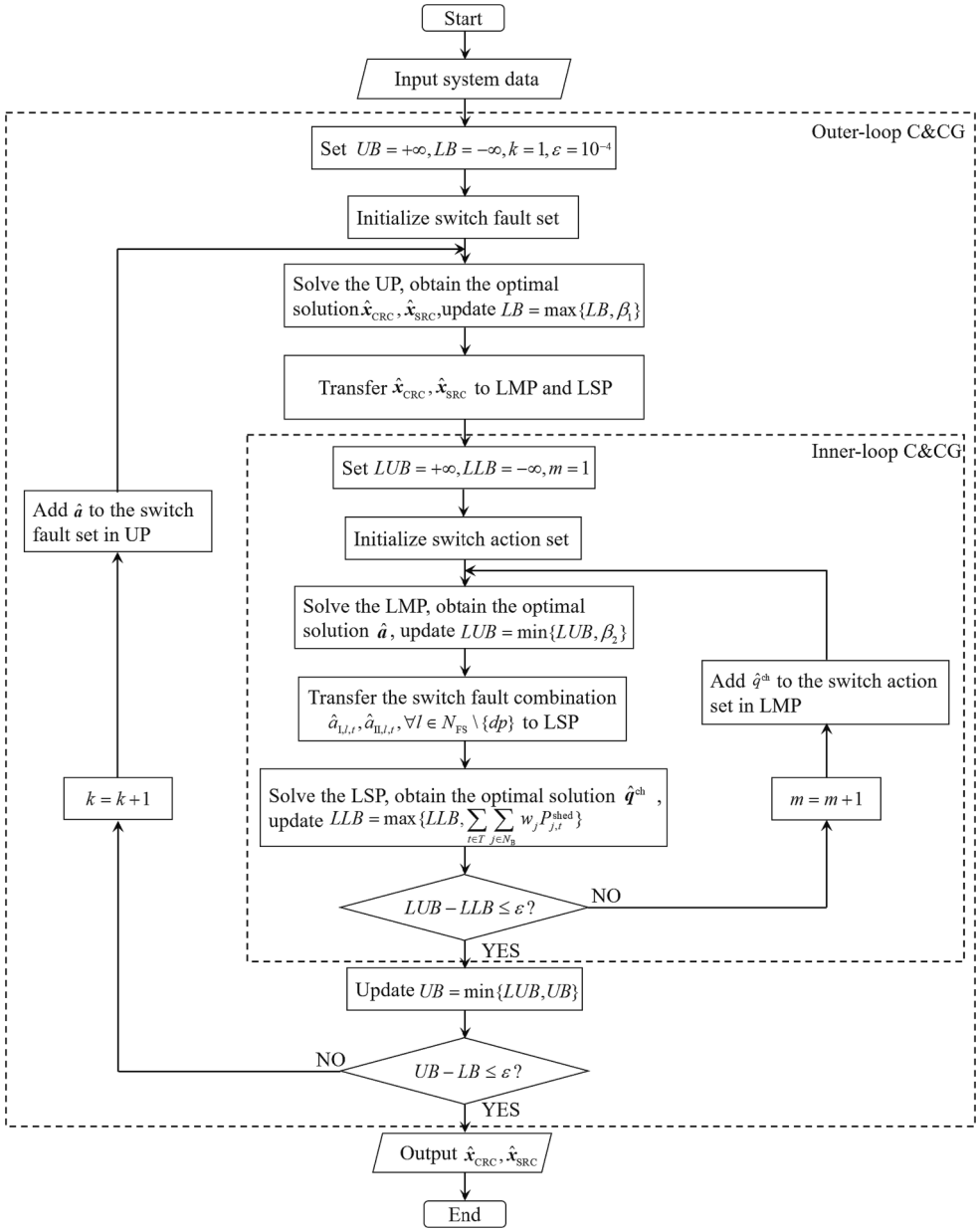

Fig. 6. The flowchart of the NC&CG algorithm.

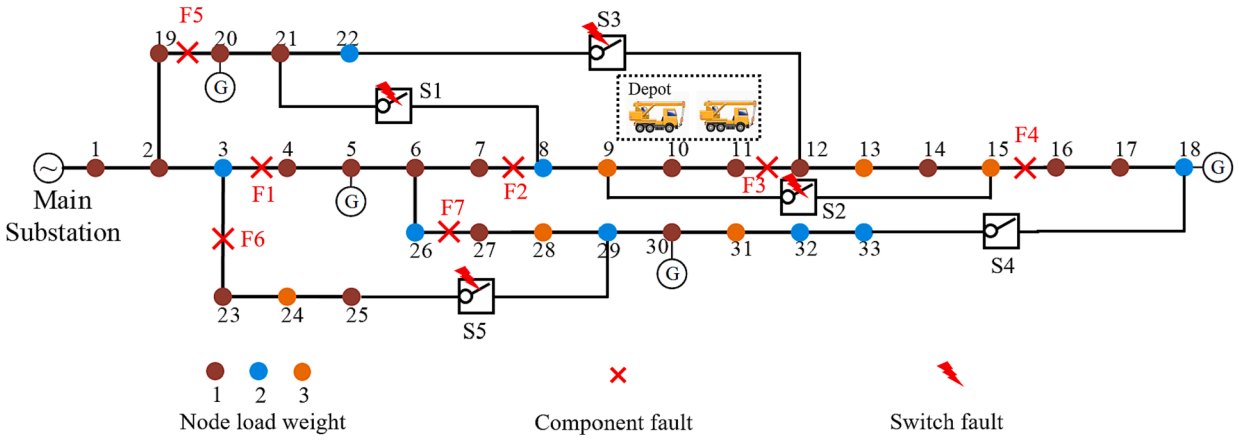

Fig. 7. The modified IEEE 33-node test system.

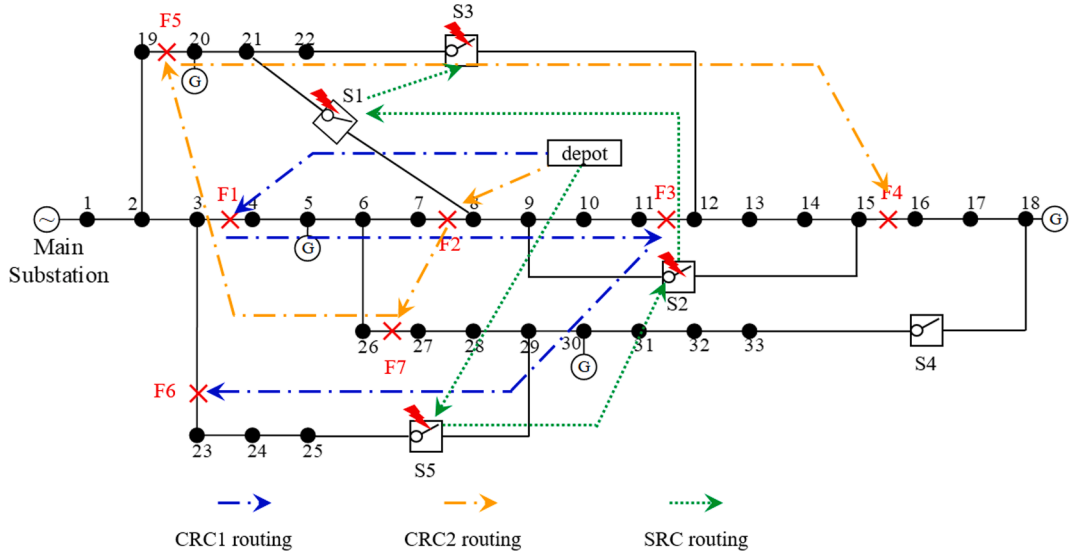

Fig. 8. The routes of CRCs and SRC.

damaged after the disaster. The repair time for each damaged line is assumed as 1 h. Besides, the disaster caused damage to four switches. The fault type of switches is unknown due to communication interruption. The repair time of fault I and fault II is set as 1.5 h and 2.5 h, respectively. Two repair crews are responsible for repairing lines, and one repair crew is dispatched to repair switches. The maximum number of fault I and fault II can be predicted based on historical data. In this case, the maximum number of fault II is set to 2.

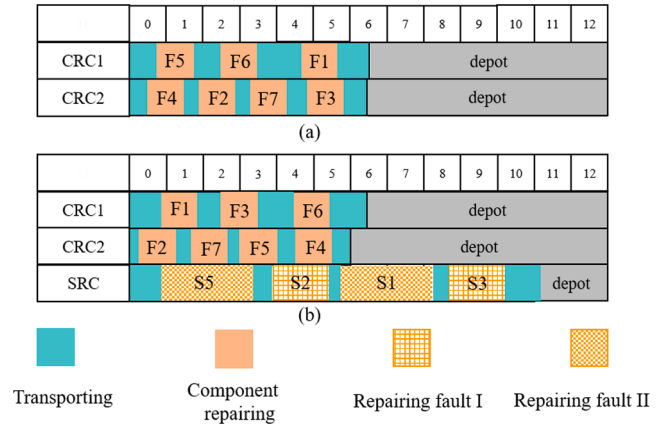

Fig. 9. Time schedule of CRCs and SRC: (a) without switch fault (b) the worst scenario.

5.2. Numerical results

After the extreme event occurs, the distribution system operator obtains the position of damaged lines and switches through fault location. Facing the uncertainty of switch faults, the operator dispatches CRCs and SRC for the worst combination of switch faults. Fig. 8 shows the routes of CRCs and SRC. The time schedule of three repair crews in the worst scenario is presented by Fig. 9. Compared with the case without the switch fault, the damage to switches greatly limits the network reconfiguration. Therefore, although the load of nodes 28–33 is more important, two CRCs gives priority to repairing F1 and F2 which

Table 1
The status of switches during the restoration.

time	S1	S2	S3	S4	S5
0	0	0	0	0	0
1–3	0	0	0	1	0
4–5	0	0	0	1	1
5–12	0	0	0	0	0

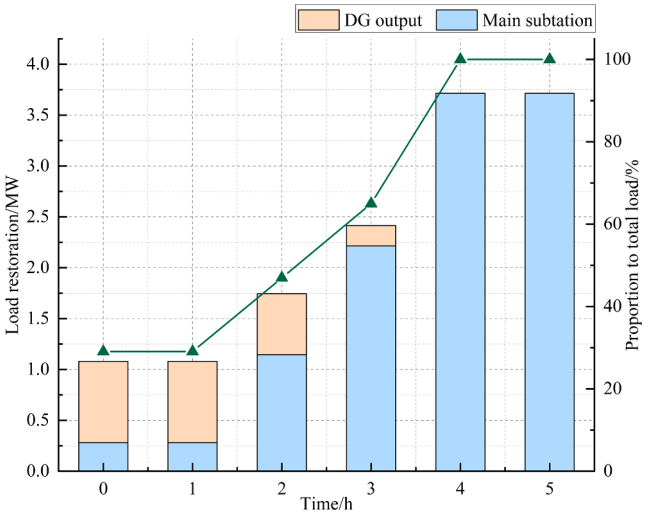

Fig. 10. Load restoration at each time step in the worst scenario.

are close to the depot, rather than F4, F5 and F6. All line faults are repaired after 5.5 h. As can be seen from the comparison of two cases, the switch fault has a significant impact on the repair crew scheduling. In coordination with the CRC scheduling, the SRC repairs S5 first. In the scheduling, SRC is expected to perform repair process II at S1 and S5.

Table 1 presents the status of each switch in the restoration process. Due to the high priority of the load at node 31, S4 is closed and the DG supplies power to node 31 at the beginning of restoration. When the maintenance of S5 is completed, the lines fault F7 has been repaired by CRC2 and the load of nodes 23–25 can be restored through S5 at $t = 4$. The status of the other three switches will not change during restoration. Therefore, it can be concluded that S4 and S5 are the most critical switches in this case.

The load restoration at each time step is shown in Fig. 10. As can be seen, the faults cause the system to lose 70 % of the load after the extreme event. The main substation begins supplying power to nodes 4–11 and nearly 45 % of the load is restored after F1 and F2 are repaired. At $t = 3$, the load of nodes 27–33 is restored due to the repair of F7. Meanwhile, the distribution network supplies power to nodes 16–18 through S4. 0.67 MW load returns to normal at $t = 3$. Because switch S5 is still in the maintenance state, so nodes 23–25 are still out of power. When S5 and F5 are repaired at $t = 4$, the system load is completely restored by network reconfiguration. The blackout lasts for 4 h, and the total loss of load is 8.54MWh during the restoration. The load restored by DGs is 2.4MWh.

5.3. The effectiveness of the proposed method in other scenarios

To test the effectiveness of the proposed scheduling method in other fault scenarios, the above robust scheduling plan is implemented in six fault scenarios which are shown in Table 2. All scenarios where the number of fault II are 2 are considered. CRCs and SRC repair each fault according to the sequence of the scheduling.

The loss of weighted load at each time step is presented in Fig. 11.

Table 2
The fault scenarios.

	Fault I	Fault II
Case1	S1,S2	S3,S5
Case2	S1,S3	S2,S5
Case3	S1,S5	S2,S3
Case4	S2,S3	S1,S5
Case5	S2,S5	S1,S3
Case6	S3,S5	S1,S2

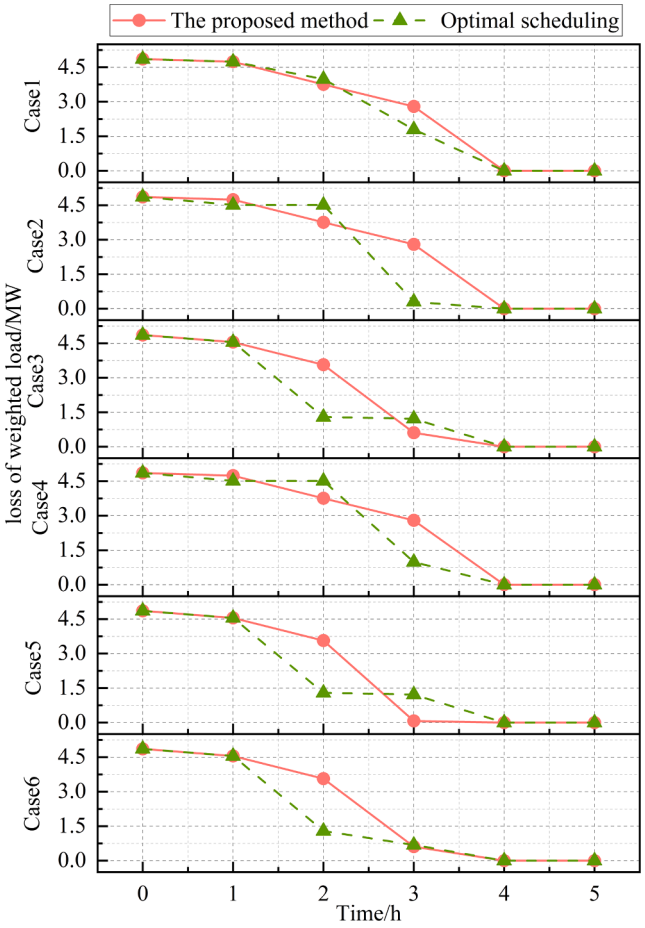

Fig. 11. Loss of weighted load at each time step in six cases.

Table 3
The comparison of the loss of weighted load(MWh).

	Optimal value	The proposed method	Without network reconfiguration
Case1	15.40	16.17	17.51
Case2	14.195	16.17	17.51
Case3	11.94	13.60	17.51
Case4	14.88	16.17	17.51
Case5	11.94	13.06	17.51
Case6	11.40	13.60	17.51

The optimal scheduling strategy is the recovery strategy formulated by the distribution system under the premise that the fault information of switches is known. The total loss in six scenarios is listed in Table 3. As shown in Fig. 11, the power outage time of the proposed method is identical to the optimal solution in most scenarios. The load shedding of the proposed method is smaller than the optimal solution at some time steps. Compared with the case without network reconfiguration, the

Table 4
The effect of six optimal scheduling strategies (MWh).

Scheduling	The loss of weighted load(MWh)					
	Case1	Case2	Case3	Case4	Case5	Case6
1	15.4	15.94	15.94	17.31	17.31	17.31
2	16.6	14.195	16.6	16.25	17.97	16.25
3	17.735	17.735	11.94	17.735	13.165	13.165
4	17.385	15.665	17.385	14.88	17.385	15.665
5	16.51	17.88	13.31	16.51	11.94	13.31
6	17.735	16.51	13.165	16.51	13.165	11.4

proposed method can reduce the load loss in all scenarios. Considering the uncertainty of fault scenarios, the scheduling strategy obtained by the proposed method needs to be applicable to all scenarios. Therefore, the scheduling strategy obtained by the proposed method may be not optimal for the single scenario. It can be observed from Table 3 that the loss of the system will increase significantly in the scenario where fault II occurs in S5. In these scenarios, the losses of the proposed method are 16.17MWh. For both of the optimal scheduling and the proposed method, the fault type of S5 directly affects the loss of the system. Therefore, it is reasonable for SRC to give priority to performing Repair II for S5. In the scenario where fault I occurs in S3, the effect of the proposed method is not superior. Because in the optimal scheduling, the SRC can arrive at S3 first and manually operate S3 to restore most of loads.

Table 4 presents the effects of each optimal scheduling strategy in six cases. The results shown in Table 4 indicate that the single-scenario optimal scheduling strategy is only effective in several specific scenarios. In some scenarios, the performance of the single-scenario optimal scheduling is even worse than that of the scheduling scheme without considering network reconfiguration. The loss of the latter is 17.51MWh. During the restoration process, the component repair plan and the switch repair plan need to cooperate with each other. The distribution system may adjust the repair sequence of lines to cooperate with the repair of switches. However, the optimal scheduling strategy only considers one scenario. If the actual fault scenario is different from the expected fault scenario, the repair of some switches may be delayed. The distribution network cannot conduct network reconfiguration as planned, resulting in the repair of some lines not contributing to load restoration. Therefore, the single-scenario optimal scheduling strategy cannot deal with all fault scenarios, and it may even be counterproductive in some scenarios. In contrast, the maximum loss of the proposed method is 16.17MWh. The results indicate that the proposed method is more effective than the single-scenario optimal scheduling strategy in the most cases.

5.4. IEEE 123-Node system

To verify the scalability of the proposed method, a further test is conducted on the larger IEEE 123-node system, as shown in Fig. 12. The system load is 3.75 MW + 2.05Mvar. The system voltage is 4.16 kV. 5 lines are installed with remote-controlled switches. The voltage range is 0.8p.u. ~ 1.2p.u. in this system. Four DGs are installed in the system, and the maximum output of each DG is 0.2 MW. The repair depot is located at node 10, and there are three repair crews in this depot. The division of repair crews, repair time, and the maximum number of fault

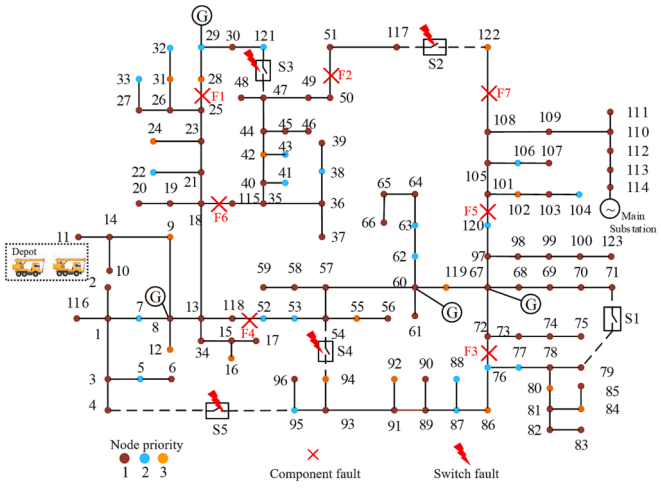

Fig. 12. The modified IEEE 123-node system.

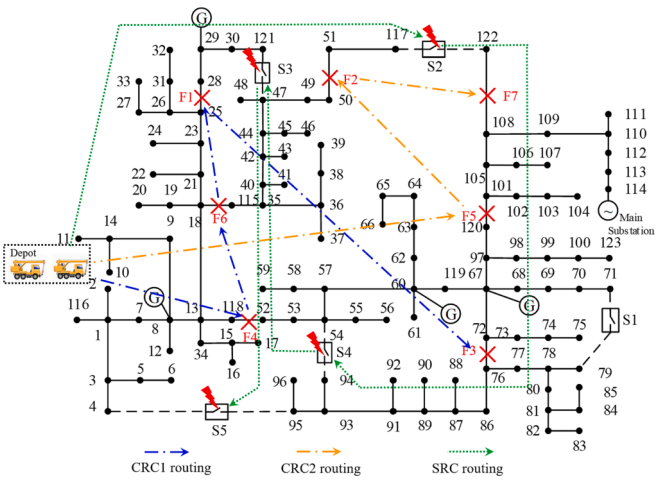

Fig. 13. The routes of CRCs and SRC in IEEE 123-node system.

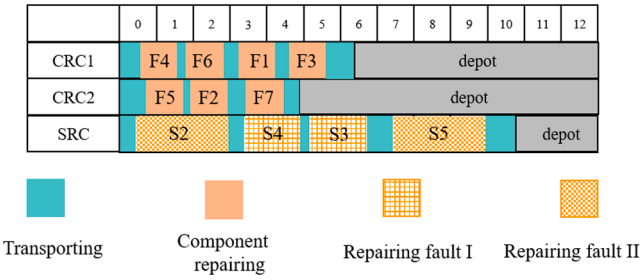

Fig. 14. Time schedule of CRCs and SRC.

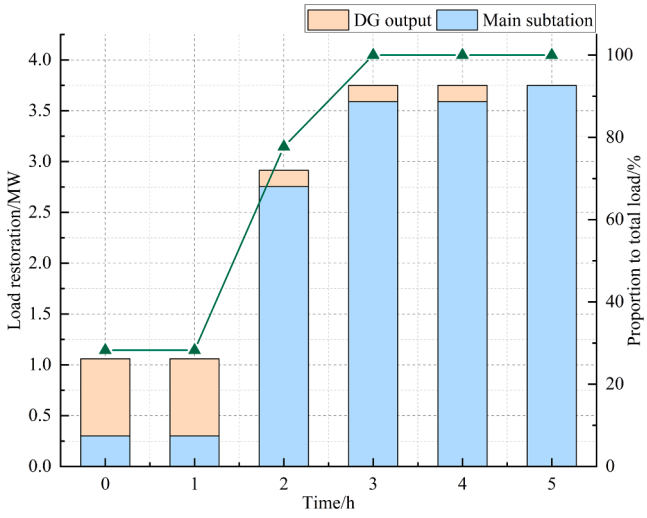

Fig. 15. Load restoration at each time step in the IEEE 123-node system.

II are the same as those in the IEEE 33-node system.

Fig. 13 shows the routes of CRCs and SRC in IEEE 123-node system. Fig. 14 shows the time schedule of CRCs and SRC. After the extreme event occurs, the switch S1 is not damaged. After F4 and F5 are repaired, the distribution network can utilize S1 to perform network reconfiguration and restore critical loads. Therefore, CRCs prioritize repairing F4 and F5. Fig. 15 shows the load restoration at each time step. It can be observed that the distribution system restores 2.34 MW load after F4 and F5 are repaired at $t = 2$. At $t = 3$, F6 and F2 are repaired by two CRCs, and switch S2 is also repaired by SRC. Although there are still faults in the distribution system, the operator can utilize network reconfiguration

Table 5
The fault scenarios.

	Fault I	Fault II
Case1	S2,S4	S3,S5
Case2	S3,S4	S2,S5
Case3	S4,S5	S2,S3
Case4	S2,S3	S4,S5
Case5	S2,S5	S3,S4
Case6	S3,S5	S2,S4

Table 6
The comparison of the loss of weighted load(MWh).

	Optimal value	The proposed method	Without network reconfiguration
Case1	8.105	8.105	10.78
Case2	8.025	8.105	10.78
Case3	7.23	8.105	10.78
Case4	7.825	8.105	10.78
Case5	7.23	8.105	10.78
Case6	7.47	8.105	10.78

and DGs to restore all loads. Component and switch repair last for 5.6 h and 9.8 h respectively. The outage time of the system is 3 h. Considering the load weight, the total loss of load is 8.105MWh. DGs play an important role during the restoration process. At the beginning of the restoration, the distribution system supplies approximately 20 % of the load through DGs. The load restored by DGs reaches 2MWh in the whole restoration process.

Similarly, the proposed scheduling plan is applied to six scenarios to test its effectiveness. Six fault scenarios are shown in Table 5. The system losses of proposed method in six scenarios are shown in Table 6. The losses of the proposed method are identical in six scenarios. Compared with the case without network reconfiguration, the proposed method reduces the load loss by 2.675MWh. Although the proposed method may not be optimal in some scenarios, the difference between the proposed method and the optimal strategy does not exceed 0.875MWh. However, calculating the optimal scheduling strategy for each scenario requires all fault information, which is an ideal case. In addition, the optimal scheduling strategy for each scenario is only applicable to specific scenarios. Table 7 presents the effectiveness of six optimal scheduling strategies in different scenarios. Notably, the proposed method has the same effect as Scheduling 1 in Case 1, but there are differences between the two scheduling schemes. The repair sequence of switches in Scheduling 1 is S4, S2, S3, S5. This difference does not affect the restoration process in Case 1. However, when the fault scenario changes, it will lead to an increase in load loss. In addition, it can be observed that the loss of some single-scenario optimal scheduling strategies exceed 10MWh in some scenarios. The results indicate that the single-scenario optimal scheduling strategy cannot effectively deal with all scenarios. In contrast, the proposed method performs stably in each scenario.

5.5. The performance of the customized NC&CG algorithm

To test the efficiency of the customized NC&CG algorithm, the proposed method is compared with a single-level model, which contains all possible fault scenarios. The single-level model is a mixed integer linear programming and can be directly solved by Gurobi. It is similar to a stochastic programming model, but its objective function is the maximum load loss in all scenarios, not the expected value of load loss in the stochastic programming model. The comparison of solution performance is presented in Table 8 The computing time of the single-level model exceeds 1800 s. In contrast, for the IEEE 33-node system, the customized NC&CG algorithm only needs to add three scenarios to find the optimal scheduling strategy. The computing time is reduced to 234 s. The scheduling strategies obtained by two models are identical. The computing time for the IEEE 123-node system is increased to 638 s, which is acceptable for the restoration. The result shows the customized NC&CG algorithm can efficiently solve the proposed tri-level robust optimization model.

Table 7
The effect of six optimal scheduling strategies.

Scheduling	The loss of weighted load(MWh)					
	Case1	Case2	Case3	Case4	Case5	Case6
1	8.105	8.345	8.345	8.225	8.225	8.345
2	8.305	8.025	8.305	8.025	8.305	8.025
3	10.14	10.14	7.23	10.14	7.23	7.23
4	8.225	8.065	8.345	7.825	8.225	8.065
5	10.26	10.38	7.47	10.26	7.23	7.47
6	10.14	10.14	7.23	10.14	7.23	7.23

Table 8
Computing time(s) of the customized NC&CG algorithm.

	The proposed method	The single-level model
IEEE 33	234	>1800
IEEE 123	638	>1800

6. Conclusion

In this paper, a robust repair crew dispatch approach considering the fault of components and remote-controlled switches is proposed to reduce system load loss. Repair crew dispatch, DG scheduling and network reconfiguration are coordinated to restore the critical load. To address the uncertainty of switches under communication interruption, the repair crew dispatch approach is formulated as a tri-level robust optimization model. To efficiently solve the proposed tri-level MILP model, a NC&CG algorithm is customized to achieve the global optimal solution. The results of numerical tests show the damage to switches has a significant impact on the restoration process. Compared with the single-scenario optimal scheduling, the robust scheduling strategy obtained by the proposed approach can effectively reduce the maximum loss of distribution system in the case with incomplete fault information. Furthermore, the customized NC&CG algorithm dramatically decreases the calculation time and efficiently achieves the global optimal solution. The proposed robust repair crew dispatch approach can improve the efficiency of restoration and reduce the system load loss. In future works, the repair crew scheduling in the case of failure of the fault location system will be studied.

CRediT authorship contribution statement

Hao Zhu: Methodology, Software, Writing – original draft. **Haipeng Xie:** Conceptualization, Writing – review & editing. **Lingfeng Tang:** Validation, Visualization. **Wei Fu:** Investigation, Data curation. **Jianlong Gao:** Resources, Supervision.

Declaration of Competing Interest

The authors declare that they have no known competing financial interests or personal relationships that could have appeared to influence the work reported in this paper.

Data availability

Data will be made available on request.

Acknowledgements

This work was supported by Natural Science Basic Research Program of Shaanxi Province (Program No. 2023-JC-QN-0480).

References

[1] Bie ZH, Lin YL, Li GF, Li FR. Battling the extreme: A study on the power system resilience. Proc IEEE 2017;105(7):1253–66. https://doi.org/10.1109/JPROC.2017.2679040.

[2] Wang YZ, Chen C, Wang JH, Baldick R. Research on resilience of power systems under natural Disasters—A review. IEEE Trans Power Syst 2016;31(2):1604–13. https://doi.org/10.1109/TPWRS.2015.2429656.

[3] Li ZY, Shahidehpour M, Aminifar F, Alabdulwahab A, Al-Turki Y. Networked microgrids for enhancing the power system resilience. Proc IEEE 2017;105(7):1289–310. https://doi.org/10.1109/JPROC.2017.2685558.

[4] Wang ZK, Ding T, Jia WH, Mu CG, Huang C, Catalao JPS. Multi-Period Restoration Model for Integrated Power-Hydrogen Systems Considering Transportation States. IEEE Trans Ind Appl 2022;58(2):2694–706. https://doi.org/10.1109/TIA.2021.3117926.

[5] Khomami MS, Jalilpoor K, Kenari MT, Sepasian MS. Bi-level network reconfiguration model to improve the resilience of distribution systems against extreme weather events. IET Gener Transm Distrib 2019;13(15):3302–10. https://doi.org/10.1049/iet-gtd.2018.6971.

[6] Liu JC, Qin C, Yu YX. Enhancing Distribution System Resilience With Proactive Islanding and RCS-Based Fast Fault Isolation and Service Restoration. IEEE Trans Smart Grid 2020;11(3):2381–95. https://doi.org/10.1109/TSG.2019.2953716.

[7] Liu JC, Yu YX, Qin C. Unified two-stage reconfiguration method for resilience enhancement of distribution systems. IET Gener Transm Distrib 2019;13(9):1734–45. https://doi.org/10.1049/iet-gtd.2018.6680.

[8] Sabouhi H, Doroudi A, Fotuhi-Firuzabad M, Bashiri M. Electricity distribution grids resilience enhancement by network reconfiguration. Int Trans Electr Energy Syst 2021;31(11). https://doi.org/10.1002/2050-7038.13047.

[9] Wu R, Sansavini G. Integrating reliability and resilience to support the transition from passive distribution grids to islanding microgrids. Appl Energy 2020;272:115254. https://doi.org/10.1016/j.apenergy.2020.115254.

[10] Hussain A, Bui V, Kim H. Microgrids as a resilience resource and strategies used by microgrids for enhancing resilience. Appl Energy 2019;240:56–72. https://doi.org/10.1016/j.apenergy.2019.02.055.

[11] Chen B, Wang J, Lu X, Chen C, Zhao S. Networked Microgrids for Grid Resilience, Robustness, and Efficiency: A Review. IEEE Trans Smart Grid 2021;12(1):18–32. https://doi.org/10.1109/TSG.2020.3010570.

[12] Shi Q, Li FX, Olama DJ, Xue Y, Starke M, Winstead C, et al. Network reconfiguration and distributed energy resource scheduling for improved distribution system resilience. Int J Electr Power Energ Syst 2021;121. https://doi.org/10.1016/j.ijepes.2020.106355.

[13] Shi Q, Li FX, Dong J, Olama M, Wang XF, Winstead C, et al. Co-optimization of repairs and dynamic network reconfiguration for improved distribution system resilience. Appl Energy 2022;318. https://doi.org/10.1016/j.apenergy.2022.119245.

[14] Wang W, Xiong XF, He YF, Hu J, Chen HZ. Scheduling of Separable Mobile Energy Storage Systems With Mobile Generators and Fuel Tankers to Boost Distribution System Resilience. IEEE Trans Smart Grid 2022;13(1):443–57. https://doi.org/10.1109/TSG.2021.3114303.

[15] Gilani M, Kazemi A, Ghasemi M. Distribution system resilience enhancement by microgrid formation considering distributed energy resources. Energy 2020;191. https://doi.org/10.1016/j.energy.2019.116442.

[16] Gilani M, Dashti R, Ghasemi M, Amirioun M, Shafie-khah M. A microgrid formation-based restoration model for resilient distribution systems using distributed energy resources and demand response programs. Sustain Cities Soc 2022;83. https://doi.org/10.1016/j.scs.2022.103975.

[17] Li XL, Chen C, Xu QW, Wen CY. Resilience for Communication Faults in Reactive Power Sharing of Microgrids. IEEE Trans Smart Grid 2021;12(4):2788–99. https://doi.org/10.1109/TSG.2021.3060917.

[18] Liu JC, Qin C, Yu YX. A Comprehensive Resilience-Oriented FLISR Method for Distribution Systems. IEEE Trans Smart Grid 2021;12(3):2136–52. https://doi.org/10.1109/TSG.2020.3047477.

[19] Teng JH, Huang WH, Luan SW. Automatic and Fast Faulted Line-Section Location Method for Distribution Systems Based on Fault Indicators. IEEE Trans Power Syst 2014;29(4):1653–62. https://doi.org/10.1109/TPWRS.2013.2294338.

[20] Galves C, Abur A. Fault Location in Power Networks Using a Sparse Set of Digital Fault Recorders. IEEE Trans Smart Grid 2022;13(5):3468–80. https://doi.org/10.1109/TSG.2022.3168904.

[21] Dehghani NL, Shafieezadeh A. Multi-Stage Resilience Management of Smart Power Distribution Systems: A Stochastic Robust Optimization Model. IEEE Trans Smart Grid 2022;13(5):3452–67. https://doi.org/10.1109/TSG.2022.3170533.

[22] Gorissen BL, Yanikoglu I, den Hertog D. A practical guide to robust optimization. Omega 2015;53:124–37. https://doi.org/10.1016/j.omega.2014.12.006.

[23] Bertsimas D, Litvinov E, Sun XA, Zhao JY, Zheng TX. Adaptive robust optimization for the security constrained unit commitment problem. IEEE Trans Power Syst 2013;28(1):52–63. https://doi.org/10.1109/TPWRS.2012.2205021.

[24] Gholami A, Shekari T, Grijalva S. Proactive management of microgrids for resiliency enhancement: An adaptive robust approach. IEEE Trans Sustain Energy 2019;10(1):470–80. https://doi.org/10.1109/TSTE.2017.2740433.

[25] Yan MY, Shahidehpour M, Paaso A, Zhang LX, Alabdulwahab A, Abusorrah A. Distribution System Resilience in Ice Storms by Optimal Routing of Mobile Devices on Congested Roads. IEEE Trans Smart Grid 2021;12(2):1314–28. https://doi.org/10.1109/TSG.2020.3036634.

[26] Lei SB, Chen C, Zhou H, Hou YH. Routing and Scheduling of Mobile Power Sources for Distribution System Resilience Enhancement. IEEE Trans Smart Grid 2019;10(5):5650–62. https://doi.org/10.1109/TSG.2018.2889347.

[27] Cai S, Xie YY, Wu QW, Xiang ZR, Jin XL, Zhang ML. Robust coordination of multiple power sources for sequential service restoration of distribution systems. Int J Electr Power Energ Syst 2021;131. https://doi.org/10.1016/j.ijepes.2021.107068.

[28] Wu H, Xie YY, Xu Y, Wu QW, Yu C, Sun JS. Robust coordination of repair and dispatch resources for post-disaster service restoration of the distribution system. Int J Electr Power Energ Syst 2021;136. https://doi.org/10.1016/j.ijepes.2021.107611.

[29] Cai S, Xie YY, Wu QW, Xiang ZR. Robust MPC-Based Microgrid Scheduling for Resilience Enhancement of Distribution System. Int J Electr Power Energ Syst 2020;121. https://doi.org/10.1016/j.ijepes.2020.106068.

[30] Sedgh SA, Doostizadeh M, Aminifar F, Shahidehpour M. Resilient-enhancing critical load restoration using mobile power sources with incomplete information. Sustain Energy Grids Netw 2021;26. https://doi.org/10.1016/j.segan.2020.100418.

[31] Dehghani NL, Shafieezadeh A. Multi-stage Resilience Management of Smart Power Distribution Systems: A Stochastic Robust Optimization Model. IEEE Trans. Smart Grid 2022; 13(5): 3452-67. https://doi.org/ 10.1109/TSG.2022.3170533.

[32] Bektas T. The multiple traveling salesman problem: An overview of formulations and solution procedures. Omega 2006;34(3):209–19. https://doi.org/10.1016/j.omega.2004.10.004.

[33] Lin YL, Chen B, Wang JH, Bie ZH. A Combined Repair Crew Dispatch Problem for Resilient Electric and Natural Gas System Considering Reconfiguration and DG Islanding. IEEE Trans Power Syst 2019;34(4):2755–67. https://doi.org/10.1109/TPWRS.2019.2895198.

[34] Yin ZY, Fang C, Yang HX, Fang YP, Xie M. Improving the resilience of power grids against typhoons with data-driven spatial distributionally robust optimization. Risk Anal 2023;43(5):979–93. https://doi.org/10.1111/risa.13995.

[35] Wang ZK, Ding T, Mu CG, Huang YH, Yang M, Yang YY, et al. A distributionally robust resilience enhancement model for transmission and distribution coordinated system using mobile energy storage and unmanned aerial vehicle. Int J Electr Power Energ Syst 2023;152. https://doi.org/10.1016/j.ijepes.2023.109256.

[36] Zhao L, Zeng B. An exact algorithm for two-stage robust optimization with mixed integer recourse problems. Report 2012.

[37] Lin YL, Bie ZH. Tri-level optimal hardening plan for a resilient distribution system considering reconfiguration and DG islanding. Appl Energy 2018;210:1266–79. https://doi.org/10.1016/j.apenergy.2017.06.059.